



Synthesis, characterization, and application of magnetic-activated carbon nanocomposite (m-Fe₃O₄@ACCs) as a new low-cost magnetic adsorbent for removal of Pb(II) from industrial wastewaters

Mohammad Reza Sovizi^{a,*}, Majid Eskandarpour^a, Morteza Afshari^b

^aDepartment of Chemistry, Maleke Ashtar University of Technology, P.O. Box 16765-3345, Tehran, Iran, Tel. +98 21 7720 3464; emails: mrsovizi@mut.ac.ir (M.R. Sovizi), mr.eskandarpour@gmail.com (M. Eskandarpour)

^bDepartment of Corrosion, Research Institute of Petroleum Industry, Tehran, Iran, email: afsharichem@gmail.com

Received 20 January 2016; Accepted 18 May 2016

ABSTRACT

In this study, magnetic-activated carbon nanocomposite (m-Fe₃O₄@ACCs), as a new adsorbent, has been prepared, characterization and used for the removal of lead ions from wastewater. Pb(II) could complexes with 4-(2-pyridylazo) resorcinol (PAR) and adsorbed onto the nanocomposite. The adsorption of Pb(II) was studied in a batch reactor at different experimental conditions such as sorbent dosage, pH of the solution, [L]/[Pb²⁺] mol ratio, contact time, and breakthrough volume and optimum values were achieved 40 mg, 11, 1:1, 15, and 450 mL, respectively. Experimental results were indicated that the m-Fe₃O₄@ACCs had removed more than 99% of Pb(II) under the optimum operational conditions. The studies on the adsorption of Pb(II) ions revealed that the process obey the pseudo-second-order kinetic model, the determining step might be chemical sorption. The adsorption of Pb(II) were found to follow the Langmuir isotherm and the maximum adsorption capacity was 239 mg/g.

Keywords: Pb(II) ion; Magnetic activated carbon nanocomposite; Removal; Adsorption

1. Introduction

Along with the development of industry and increasing use of lead over the past few decades led to an increased pollution of Pb(II) ions in natural water and wastewater and posed serious environmental and health risks [1]. The main sources of Pb(II) ions release into the environment from industry include lead fabrications, batteries, gasoline, paints, pigments, metal corrosion and so on [2,3]. Lead is accumulated in humans and animals tissues and damage to the kidney, nervous system, reproductive system, liver and

brain and may bring serious health problems such as sterility, abortion, stillbirths, and neonatal deaths [4]. The reach of lead level to more than 0.5 µg/mL in the blood causes difference abnormalities. It interferes in the metabolism of calcium and vitamin D and affects formation of hemoglobin and causes anemia [5]. According to US Environmental Protection Agency, the maximum contaminant level for Pb(II) in drinking water is 0.015 mg/L [6].

Due to the problems mentioned above, in recent years, many researchers interested has been development of proper method for Pb(II) removal from water and wastewaters [7]. Various absorbents include of

*Corresponding author.

modified silica [8], hydroxyapatite and ferrihydrite [9], modified chitosan [10,11] corn straw [12], nanoalginate-based biosorbent [13], immobilized materials [14,15], modified iron oxide [6], ion-imprinted [16,17], graphene oxide [18–21], surfactant-modified [22], zero-valent [23,24], modified polyvinyl alcohol [25], biosorption [26,27], functionalized-MnO₂/chitosan nanocomposites [28], gelation with alginate [29], SBA-15 modified [30], cellulose-based adsorbents [31], polyampholyte hydrogel [32], and carbon nanotube-based composites [33–37] have been proposed for Pb(II) removal.

Activated carbons (ACs) are the most common adsorbents for metal ions [38–40]. Unfortunately, the use of ACs in large scale is limited because they are notoriously difficult to separate from solution [41]. A combination between carbon active and nanoparticles iron oxide can create a new adsorbent named magnetic nanocomposites, which will possess easy recovery from treated effluents by applying magnet [42,43]. In this magnetic-activated carbon nanocomposite (m-Fe₃O₄@ACCs), it has a special structure with functionalized carbon as an outer shell and magnetite as an inner core.

Magnetic nanocomposites have preferable advantages over conventional adsorbents [44] because of favorable water dispersibility their strong magnetic responsiveness and benign biocompatibility [45,46]. This composites have been applied in many fields including analytical chemistry, bioscience, magnetic resonance imaging, and pollutants removal [47].

The present study aimed to investigate the adsorptive removal of Pb(II) ions from water and wastewater using magnetic-activated carbon nanocomposite (m-Fe₃O₄@ACCs). Regular-shaped nanocomposites were prepared via a coprecipitation method in laboratory and comprehensively characterized with X-ray diffraction, Brunauer–Emmett–Teller (BET), thermogravimetric analysis (TGA), scanning electron microscopy (SEM) and vibrating sample magnetometer (VSM). For increasing adsorption efficiency, Pb(II) ions reacted with 4-(2-pyridylazo) resorcinol (PAR) ligand (Fig. 1) [48] and the formed complexes were adsorbed onto the nanocomposite.

The effect of some parameters, such as Pb(II) ions initial concentration, contact time, temperature, adsorbent dosage, and pH, were investigated on the adsorption efficiency of Pb(II) ions from aqueous solutions onto m-Fe₃O₄@ACCs. Additionally, adsorption isotherms, kinetic and thermodynamic parameters were also evaluated. The information gained in this study could be useful for both designing low-cost, easily available adsorbents based on ACs and further practical applications in other inorganic ions removal from water and wastewaters.

2. Materials and methods

2.1. Standard solutions and reagents

All chemicals were analytical reagent grade and were obtained from Merck (Darmstadt, Germany; www.merck-chemicals.com) and solutions were prepared with high purity water. A stock solution of 1,000 mg/L of lead was prepared by dissolving 0.1077 g of PbO in nitric acid and diluting to 100 mL with water. More dilute standard solutions were prepared daily by diluting the stock solutions. The ligand solution (1,000 mg/L) was prepared by dissolving analytical reagent grade 4-(2-Pyridylazo) resorcinol (PAR) in high-purity water. The pH of solutions was adjusted by dropwise addition of NH₃ (0.1 mg/L) and HCl (0.1 mg/L). Deionized (DI) water (Millipore ultra-pure system with millipak express filter, USA) was used throughout of the study. Prior to use, all glassware were rinsed with sulfochromic acid solution and three times with deionized water.

2.2. Instrumentation

A UV–vis spectrophotometer (Hitachi U-3310, Tokyo, Japan; www.hitachi.com) equipped with a 1-cm quartz cell and was used for recording the visible spectra and absorbance measurements in $\lambda_{\max} = 520$ nm in parameters optimization, and for lead determination in real samples, the measurements were performed with a Perkin–Elmer Optima 2100 DV simultaneous inductively coupled plasma optical

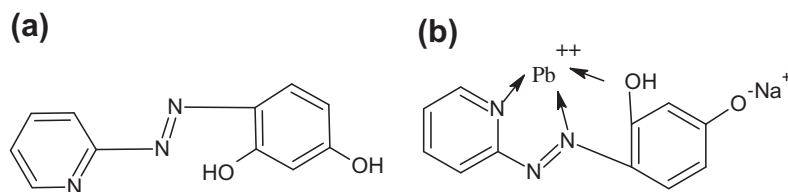


Fig. 1. (a) 4-(2-Pyridylazo) resorcinol (PAR) and (b) PAR–Pb(II) complex.

emission spectrometry (ICP-OES) (Shelton, USA; www.perkinelmer.com) coupled to a pneumatic nebulizer and equipped with a charge coupled device. Operational conditions and selected wavelengths for the Pb^{2+} ions were optimized and summarized in Table 1.

The pH of solutions was measured by a Corning ion analyzer 255 pH meter (New York, USA; www.corning.com) with combined glass electrode supplied with a combined glass-calomel electrode. Transmission electron microscopy (TEM) images of the magnetic nanocomposite were obtained with a Philips CM120 transmission electron microscope (Eindhoven, Netherlands; www.fei.com) and TGA of the adsorbent was performed by FTDA/TGA instrument from Mettler Toledo (Boston, England; www.mt.com/lab). The magnetic properties of the nanocomposite were measured using a homemade VSM (University of Esfahan, Iran). The high-purity water was prepared on a Millipore water purification system (Billerica, MA, USA; www.millipore.com). A super magnet Nd–Fe–B (1.4 T, 10 cm × 5 cm × 2 cm) was used for sorbent separation from solution.

2.3. Preparation and characterization of magnetic-activated carbon nanocomposite (m-Fe₃O₄@ACCs)

The magnetic nanocomposite was prepared based on the method that was described by Tajabadi et al. [49]. At the first step, AC was modified with nitric acid (65%) for 3 h at 80°C to make it hydrophilic. Then, 1 g of the modified AC was dispersed in 40 mL aqueous solution containing 8 g Fe(NO₃)₃·9H₂O and stirred for 45 min. The resulted mixture filtrated and dried. Afterward, modified AC that adsorbed iron salt was heated at 750°C for 3 h in the presence of argon for the formation of magnetic nanoparticles of Fe₃O₄ that are obtained by combustion synthesis in the pores

of AC [50]. The obtained AC based on magnetic nanocomposite was stable under environmental conditions for several months. TEM image of the prepared m-Fe₃O₄@ACCs that is shown in Fig. 2(a) demonstrates the existence of iron oxide nanoparticles with diameter of about 40–80 nm. The magnetic hysteresis loop of m-Fe₃O₄@ACCs that was measured by VSM is shown in Fig. 2(b). From the plotting of magnetization (M) versus magnetic field (H), very weak hysteresis revealed the resultant magnetic nanoparticles were nearly super paramagnetic with a saturation magnetization (M_s) of 7.28 emu/g at room temperature. TGA of the magnetic nanoparticles (Fig. 2(c)) indicated that there was about 10 wt% of iron oxide inside the synthesized nanocomposite.

2.4. Removal procedure

An aliquot of 25 mL solution (pH 11.0) contain known concentration of lead, was transferred to 50-mL glass beaker. Then PAR (1:1 ratio with Pb(II)) and sorbent were added and shaken completely. The mixtures were stirred and allowed to complete the extraction process for 30 min. Subsequently, an Nd–Fe–B strong magnet (10 cm × 5 cm × 4 cm, 1.47 T) was placed at the bottom of the beaker and the magnetic adsorbent was collected from the solutions.

After about 5 min, the solutions became clear and supernatant solutions were decanted. Finally, absorption of Pb²⁺ complex was measured by UV/vis spectrophotometer at $\lambda_{max} = 520$ nm. The lead removal efficiency of m-Fe₃O₄@ACCs was calculated by using the following equation:

$$\% \text{ Removal efficiency} = \frac{C_0 - C_{eq}}{C_0} \times 100 \quad (1)$$

where C_0 and C_{eq} represent the Pb(II) concentrations (mg/L) before and after adsorption in solution, respectively [51].

The affected of various parameters such as pH solution, contact time, adsorbent dosage, mol ratio of PAR to lead and breakthrough volume affected on removal efficiencies of lead from aqueous solutions by magnetic activated carbon nanocomposite (m-Fe₃O₄@ACCs) adsorbents were investigated and optimized.

2.5. Removing of lead ion from real samples

The proposed procedure was applied to the removal of lead ions in real samples such as top water, Isfahan steel company's wastewater (lead concentration in waste water was 0.03 mg/L) and Tehran

Table 1
The optimum instrumental conditions of ICP-OES

Parameter	Characteristics
Plasma	Gas Argon
Plasma gas flow rate	12 L/min
Auxiliary gas flow rate	0.3 L/min
Frequency of RF generator	40 MHz
RF generator power	1,300 W
Observation height	8 mm
Nebulizer pressure	1.8 L/min
Eluent deionized	Water
Elution rate	5 mL/min
Pb wavelength (nm)	220.353

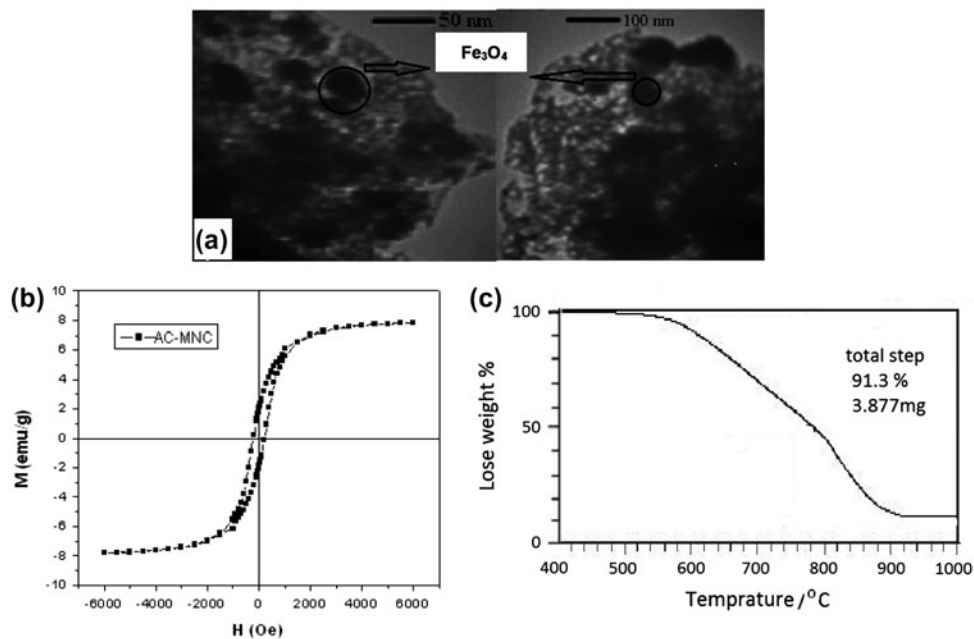


Fig. 2. (a) TEM image, (b) magnetic hysteresis cycles and (c) TGA analysis of the synthesized m-Fe₃O₄@ACCs.

battery manufacturing industrial wastewater. The sample were collected for 25 d, filtered with qualitative filter papers (4.25 cm diameters, 20–25 μm pore size) to remove suspended particulate matter and maintained in refrigerator (4 $^{\circ}\text{C}$) and above procedure was followed. Lead remaining in the samples after removal process was determined by inductively coupled plasma optical emission spectroscopy (ICP-OES) technique.

3. Results and discussion

3.1. Lead adsorption

3.1.1. Effect of pH

pH is one of the most important parameters controlling uptake of heavy metals from wastewater and aqueous solutions [52,53]. Fig. 3 shows the effect of pH on lead removal efficiencies of m-Fe₃O₄@ACCs.

As can be seen from Fig. 3, by increasing of solution pH from 4.0 to 11.0, the lead removal increase from 20 to 88%, that's mean the Pb(II) adsorption capacity and removal efficiency increased with

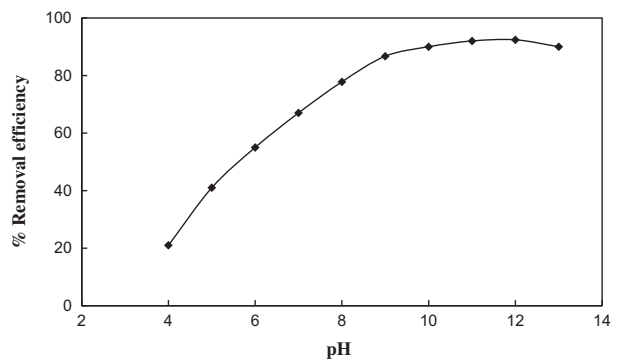


Fig. 3. Effect of pH on the removal of Pb(II).

Notes: Experimental conditions: volume = 25 mL, [Pb²⁺] = 25 mg/L, [62] = 25 mg/L, amount of sorbent = 10 mg, stirring time = 30 min.

increasing of pH. The effects of pH can be investigated from two aspects, effect on complexation between PAR and Pb(II) and effect on adsorbent surface charge. The first effect explained by optimum pH for complexation of the lead ions with PAR (pH 10.0) [48].

Adsorbent	Acidic	Neutral	Basic
Carbon	$-\text{COOH} + \text{H}^+ \leftrightarrow -\text{COOH}_2^+$	$-\text{COOH}$	$-\text{COOH} + \text{OH}^- \leftrightarrow -\text{COO}^-$
Carbon	$-\text{COH} + \text{H}^+ \leftrightarrow -\text{COH}_2^+$	$-\text{COH}$	$-\text{COH} + \text{OH}^- \leftrightarrow -\text{CO}^-$
Metal oxide	$-\text{MOH} + \text{H}^+ \leftrightarrow -\text{MOH}_2^+$	$-\text{MOH}$	$-\text{MOH} + \text{OH}^- \leftrightarrow -\text{MO}^-$

The adsorption affinity of $m\text{-Fe}_3\text{O}_4@\text{ACCs}$ was impacted significantly by the physicochemical properties of adsorbent and lead ions (include complexes) under given pH. The hydroxyl and carboxylated groups on the surface of adsorbent (carbon and metal oxide) in different pH were modeled as below [54].

Due to existence of carboxylic group on the surface of $m\text{-Fe}_3\text{O}_4@\text{ACCs}$, the surface charge of $m\text{-Fe}_3\text{O}_4@\text{ACCs}$ became negative by increasing of pH and electrostatic attraction occurred between the positively charged metal ions complexes ($\text{Pb}(\text{NH}_3)_4^{2+}$ and $\text{PAR}\text{-Pb}(\text{II})$) and the adsorbent particles. At $\text{pH} > 11.0$, the electrostatic and hydrophobic interactions reached to maximum value and amount of removal and extraction efficiency was constant, thus $\text{pH} 11.0$ was chosen for further studies.

3.1.2. $[\text{L}]/[\text{Pb}^{2+}]$ mol ratio

Fig. 4 shows the effect of $[\text{L}]/[\text{Pb}^{2+}]$ mol ratio on Pb(II) removal efficiencies by $m\text{-Fe}_3\text{O}_4@\text{ACCs}$. In the absence of PAR, the lead removal by sorbent was 55%. This removal can be explained by electrostatic attraction between the positively charged metal ion–ammonium complexes (Pb^{2+} , $\text{Pb}(\text{NH}_3)_4^{2+}$) and adsorbent particles. With PAR adding in solution and forming the $\text{PAR}\text{-Pb}^{2+}$ complex, due to hydrophobic interactions between complex and adsorbent, the removal efficiency was increasing from 55 to 89%. By increasing in mol ratio of $[\text{L}]/[\text{Pb}^{2+}]$, the lead removal efficiency decreased due to competition adsorption between the free ligand and complexes on the sorbent. In most cases, it has been reported that addition of ligand more than is stoichiometrically could be inhibit the adsorption of metal ions and complexes by the sorbent [55].

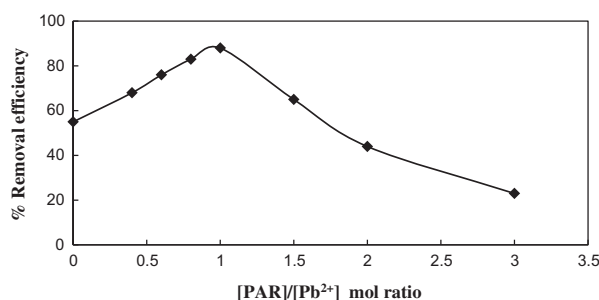


Fig. 4. Effect of $[\text{62}]/[\text{Pb}^{2+}]$ ratio on the removal of Pb(II) efficiencies.

Notes: Experimental conditions: volume = 25 mL, $[\text{Pb}^{2+}] = 25$ mg/L, $[\text{62}] = 25$ mg/L, amount of sorbent = 10 mg, stirring time 30 min, $\text{pH} 11$.

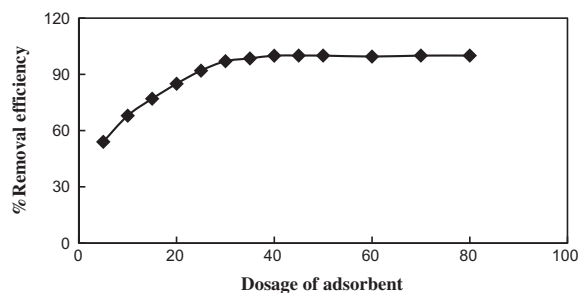


Fig. 5. Effect of MNC-AC dosage on the removal of Pb(II) efficiencies.

Notes: Experimental conditions: volume = 25 mL, $[\text{Pb}^{2+}] = 25$ mg/L, $[\text{62}] = 25$ mg/L, stirring time = 30 min, $\text{pH} 11$.

3.1.3. Effect of sorbent dosage

The effect of $m\text{-Fe}_3\text{O}_4@\text{ACCs}$ amount on the removal of lead was investigated using a batch technique by adding a known quantity of the nanocomposite in the range of 5–80 mg (Fig. 5). The percent removal of lead increased with increasing $m\text{-Fe}_3\text{O}_4@\text{ACCs}$ dosage up to 30 mg and eventually reached to a value of 98%. This observation can be explained by the greater number of adsorption sites available for Pb(II) [56]. Further increase in the adsorbent dosage did not affect the removal of lead. Therefore, the optimum dosage of $m\text{-Fe}_3\text{O}_4@\text{ACCs}$ for removing lead from their individual solutions was found to be 40 mg.

3.1.4. Effect of contact time

The contact time between adsorbate and adsorbent is one of the most important design parameters that effect on the performance of adsorption processes [56]. Fig. 6 shows removal efficiencies as a function of

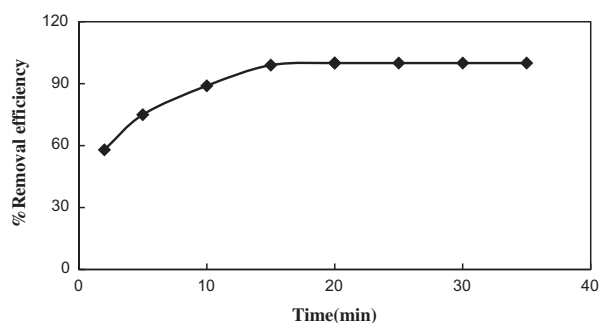


Fig. 6. Effect of contact time on the removal of Pb(II) efficiencies.

Notes: Experimental conditions: $[\text{Pb}^{2+}] = 25$ mg/L, $[\text{62}] = 25$ mg/L, $\text{pH} 11$, amount of sorbent = 40 mg, volume solution = 450 mL.

stirring time ranging between 2 and 35 min. These figure showed that adsorption process started immediately after adding m-Fe₃O₄@ACCs to solutions. The removal efficiency rapidly increased from 58% in the first minute of contact to a value of 99% where the equilibrium condition was attained after 15 min. Because shorter contact times in an adsorption system have lower capital and operational costs for real-world applications, therefore 15 min was selected for optimum contact time between sample solution and m-Fe₃O₄@ACCs nanocomposite.

3.1.5. Effect of volume sample solutions (breakthrough volume)

In removing process, the sample volume is one of important factor. In order to obtain higher removal factor, the ratio of sample to eluent volumes should be increased by lowering the eluent volume and/or increasing the sample volume [57]. Therefore, the maximum applicable sample solution was investigated by using increasing volume of metal ion solution and keeping the total amount of metal ions constant at 1 mg. The effect of aqueous phase volume on the removal lead from aqueous solutions was studied in the range 25–600 mL. It was found that the dilution effect was not significant for the sample volumes up to 450 mL for lead removal efficiency (Fig. 7). At higher sample volumes, the removal efficiency decreased gradually with increasing volume of sample solution.

3.1.6. Effect of interfering ions

The effects of common interference ions on the sorption of Pb(II) by m-Fe₃O₄@ACCs were investigated. In these experiments, the solutions of 10 mg/L

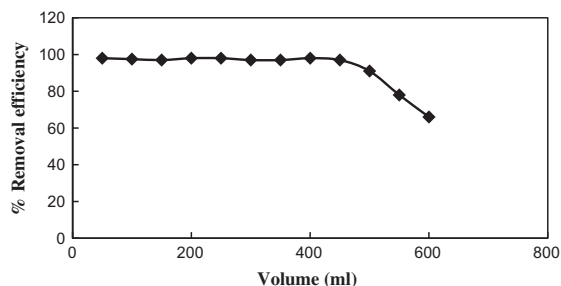


Fig. 7. Effect of aqueous phase volume on the removal of Pb(II) efficiencies.

Notes: Experimental conditions: [Pb²⁺] = 25 mg/L, [62] = 25 mg/L, stirring time = 30 min, pH 11, amount of sorbent = 40 mg.

Pb(II) containing the interfering ions were treated according to the recommended procedure. A series of selected cations and anions was used to study and evaluate their interfering effects on the sorption processes of Pb(II) by m-Fe₃O₄@ACCs. The selected anions were Cl⁻, NO₃⁻, and SO₄²⁻ and the selected cations were Na⁺, K⁺, Al³⁺, Ca²⁺, Ba²⁺, Co²⁺, Ni²⁺, Zn²⁺, Cu²⁺, Cd²⁺, and Mg²⁺. The tolerance limits of the coexisting ions defined as the largest amount making the recovery of Pb less than 95%. The data listed (Table 2) are clearly showing that some of the selected cations and anions such as (Na⁺, K⁺, Al³⁺, Ca²⁺, Ca²⁺, Cl⁻, NO₃⁻, and SO₄²⁻) no significant influence on the removal of Pb(II) ion under the selected conditions. However, Co²⁺, Ni²⁺, and Cu²⁺ were found to exhibit high interference in Pb(II) extraction by m-Fe₃O₄@ACCs because they have same trends and behavior for complexation with PAR and adsorption onto m-Fe₃O₄@ACCs.

3.1.7. Desorption and reusability studies

For express the cost effective of proposed method, potential applications, the regeneration and reusability of an adsorbent are important factors that should be expressed. Possible desorption of lead ion was investigated by using different solutions such as pure methanol, pure ethanol, mixed methanol/acetic acid solution (with different volume ratios of 1:1, 2:1, and 1:2), mixed water/acetic acid solution (with different volume ratios of 1:1, 1:2, and 2:1), Nitric acid and hydrochloridric acid. The study revealed that the adsorbed lead could be completely desorbed in the presence of mixed water/acetic acid solution with a volume ratio of 1:1. In this study, more than 98% of proposed lead could be desorbed and recovered by 1 mL of mixed water/acetic acid solution with a volume ratio of 1:1 in 25 min, when 0.45 mg Pb(II)

Table 2

Effect of interfering ions on metal sorption capacity of Pb(II)

Interference ion	Ratio of interference ion on lead ([In]/[Pb ²⁺])	% Removal
Cu ²⁺	1	60.0
Ni ²⁺ , Co ²⁺	2	87.1
Zn ²⁺	10	92.2
Cd ²⁺ , Mg ²⁺	50	94.8
Al ³⁺	100	97.3
Ba ²⁺ , Ca ²⁺	400	95.2
Na ⁺ , K ⁺	500	96.3
Cl ⁻ , NO ₃ ⁻ , SO ₄ ²⁻	1,000	97.4

(450 mL with a concentration of 1 mg/L) was already adsorbed on m-Fe₃O₄@ACCs. The reusability of the adsorbents in several successive separation processes was tested and the result showed that the m-Fe₃O₄@ACCs can be recycled and reused for seven times without significant reduction in its removal efficiency.

3.1.8. Removing of lead ion from water and wastewater

The proposed procedure was applied to the removal of lead ion in real samples such as top water, Isfahan steel company's wastewater (lead concentration in waste water was 0.03 mg/L) and Tehran battery manufacturing industrial wastewater. As can be seen in Table 3, the proposed method could be successfully applied for the removing of lead in real aqueous solution.

3.2. Kinetic study

In order to understand sorption kinetics of lead ion on m-Fe₃O₄@ACCs, pseudo-first-order kinetic and pseudo-second-order kinetic were applied to experimental data. In fact, examine the mechanism of adsorption process such as mass transfer and chemical reaction, a suitable kinetic model is needed to analyze the adsorption data. In removing process, pseudo-first-order and pseudo-second-order kinetic models have been extensively used to describe the transport of metal ions inside the adsorbents [58]. The conformity between experimental data coefficient and the model predicted values was expressed by the correlation coefficient. The amount of lead ion adsorbed per unit mass of the adsorbent was determined from the following expression:

Table 3

The application of presented method for removal of Pb(II) from real sample ($n = 3$)

Sample	Added (μg)	% Removal
Top water	0	99 ± 1
	50	99 ± 2
	100	98 ± 2
Wastewater (Isfahan steel company's wastewater)	0	99 ± 2
	20	99 ± 2
	50	94 ± 3
Wastewater (Tehran battery manufacturing industrial wastewater)	0	98 ± 2
	20	94 ± 3
	50	90 ± 3

$$q_e = \frac{(C_0 - C_e)V}{m} \quad (2)$$

where q_e is the amount of adsorbed per unit mass of the adsorbent at equilibrium time (mg/g), C_0 and C_e are the initial and equilibrium concentrations (mg/L), respectively and m is the mass of the adsorbent (g) and V is the volume of the solution (L).

The adsorption kinetics may be described by a pseudo-first-order equation. The change in concentration of the system can be expressed using the following equation:

$$\frac{dq_t}{dt} = K_1(q_e - q_t) \quad (3)$$

After integration by applying the initial condition at $t = 0$, $q_t = 0$ and rearrangement of equation, it can be presented as a follows:

$$\log(q_e - q_t) = \log q_e - \frac{K_1 t}{2.303} \quad (4)$$

where q_t is adsorption capacity (mg/g), at any time, and K_1 is the rate constant.

The adsorption kinetics by m-Fe₃O₄@ACCs may be described by a pseudo-second-order equation. The differential equation can be described as a follows:

$$\frac{dq_t}{dt} = K_2(q_e - q_t)^2 \quad (5)$$

By integrating the above equation and applying the initial condition of $t = 0$, $q_t = 0$, the following equation can be arrangement to obtain a linear form:

$$\frac{t}{q_t} = \frac{1}{K_2 q_e^2} + \frac{t}{q_e} \quad (6)$$

where K_2 (g/mg min) is rate constant pseudo-second-order adsorption [52].

The adsorption of Pb(II) on m-Fe₃O₄@ACCs as a function of contact time (1–40 min) in different initial metal concentrations shown in Fig. 8.

A close look at Fig. 8 reveals that the adsorption occurs quickly during the early stage of adsorption reaction. The adsorption of Pb(II) (q_t) increased with increasing contact time and rapid sorption was observed during the first 5 min of contact time that may be due to the plenty of availability active sites in the

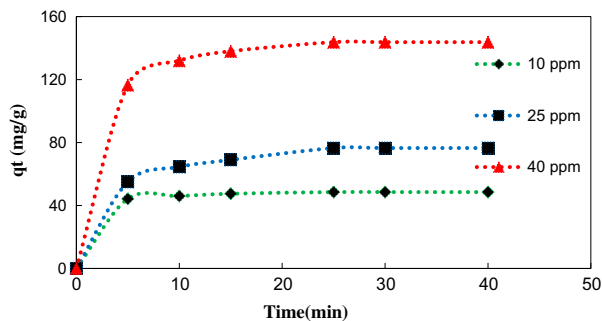


Fig. 8. Adsorption capacity-time for Pb(II) removal by m-Fe₃O₄@ACCs.

sorbents. About 15 min of contact time was sufficient to achieve this state and further increase in contact time did not significant change on the adsorption of Pb(II). A change in initial metal ion concentration from 10 to 40 mg/L caused an increase in the amount of adsorbed lead complexes (PAR-Pb²⁺ and Pb(NH₃)₄²⁺). This could be due to the increase in the driving force to overcome all mass transfer resistance of metal ions between the aqueous and solid phases [59].

The intercept of each plot in Figs. 7 and 8 are used to calculate the adsorption rate constants (K_1 and K_2) and the amount of adsorption in equilibrium (q_e). The calculated kinetics parameters for adsorption of Pb(II) ions onto the m-Fe₃O₄@ACCs at three initial concentrations of Pb(II) ions are listed in Table 4. As can be observed, at all initial concentration of Pb(II) ions, the correlation coefficients (R^2) of the pseudo-second-order kinetics model are higher than those of the pseudo-first-order kinetics model.

Also, the experimental q_e values are closer to q_e values calculated from the pseudo-second-order kinetic model. The consistency of the experimental data with the pseudo-second-order kinetic model indicates that the adsorption of Pb(II) ions onto the m-Fe₃O₄@ACCs at all concentration is controlled by chemical adsorption (chemisorption) involving valence forces through sharing or exchange electrons between sorbent and sorbate. In chemical adsorption, it is assumed that the adsorption capacity is proportional to the number of active sites occupied on the adsorbent surface [60].

By this model, it can be assumed that the adsorption occurred through chemisorptions and the adsorption followed a monolayer regime on the adsorbent surface. Also, the adsorption phenomena might include the valence forces through sharing electrons between Pb(II) ions and m-Fe₃O₄@ACCs [6].

3.3. Adsorption isotherms

The adsorption isotherm provides information between concentrations of metal ions in solution (C_{eq} ; mg/L) and the amount of adsorbed metal ions on adsorbent (q_{eq} ; mg/g) at equilibrium state. Langmuir and Freundlich adsorption isotherms were used to fit to the experimental data [59]. Linear regression was frequently used to determine the most fitted model throughout the years and the method of least squares has been frequently used for finding the parameters of the models. However, transformations of nonlinear forms to linear isotherm equations implicitly alter their error structure and may also violate the error variance and normality assumptions of standard least squares [61]. In this study, we used linear and nonlinear method for describe the equilibrium state data.

Langmuir model assumes uniform adsorption on the surface and is valid for a monolayer sorption with a homogeneous distribution of the sorption sites and sorption energies:

$$q_e = \frac{K_1 q_m C_e}{1 + K_L C_e} \quad (7)$$

Eq. (7) could be explained in linear form:

$$\frac{1}{q_e} = \frac{1}{q_m} + \frac{1}{K_L q_m C_e} \quad (8)$$

That C_e (mg/L) and q_e (mg/g) are the concentrations of sorbate and the amount of sorbate adsorbed at equilibrium, and K_L is the Langmuir's constant that related to the energy of adsorption.

Freundlich isotherm model can be used to description the sorption on heterogeneous surfaces as well as a multilayer sorption. It assumption states that the ion adsorption occurs on a heterogeneous adsorbent surface. Freundlich model is expressed as follows:

$$q_e = K_F C_e^{1/n} \quad (9)$$

The logarithmic form of the equation is expressed as follows:

$$\log q_e = \log K_F + \frac{1}{n} \log C_e \quad (10)$$

where K_F is the Freundlich constant and $1/n$ is the empirical constant indicating adsorption intensity

Table 4

The constant parameters of pseudo-first-order and pseudo-second-order models

Concentration (mg/L)	q_{exp}	Pseudo-first-order			Pseudo-second-order		
		q_{cal1}	K_1	R^2	q_{cal2}	K_2	R^2
10	47	7.9	0.13	0.9521	50	0.0061	0.9979
25	77	22.4	0.06	0.8575	83	0.0083	0.9998
40	145	50.5	0.10	0.9199	156	0.0056	0.9997

that depends on the temperature and properties of the sorbate and the sorbent [34]. The sorption isotherms of lead ion on m-Fe₃O₄@ACCs are shown in Fig. 9.

The adsorption behavior of Pb(II) on the m-Fe₃O₄@ACCs expressed by Langmuir isotherm linear model gives the following equation:

$$\frac{C_e}{q_e} = 0.0041C_e + 0.073 \quad (r^2 = 0.9939) \quad (11)$$

By using this equation, maximum adsorption capacity calculated from the slope was 243.9 mg/g. From the fitting curves in Fig. 9 and the correlation coefficients listed in Table 5, it is clear that the Langmuir model simulates the experimental data better than the Freundlich model. This in turn suggests that adsorption occurs as the monolayer lead adsorb onto the homogeneous adsorbent surface.

Maximum monolayer the sorption capacity (q_m) was calculated from Langmuir model as 243.9 mg/g (Table 5). The maximum sorption capacities for lead removal by various species are given in Table 6. For comparison that show the magnetic activated carbon

nanocomposite (m-Fe₃O₄@ACCs) have high capacity for the removal of Pb(II) from aqueous solution. As mentioned, the high capacity related to electrostatic and hydrophobic interaction between the lead complexes (PAR-Pb²⁺ and Pb(NH₃)₄²⁺) and m-Fe₃O₄@ACCs.

3.4. Desorption and reusability studies

To express the cost effective of proposed method, potential applications, the regeneration and reusability of an adsorbent are important factors that should be expressed. Possible desorption of lead ion was investigated by using different solutions such as pure methanol, pure ethanol, mixed methanol/acetic acid solution (with different volume ratios of 1:1, 2:1, and 1:2), mixed water/acetic acid solution (with different volume ratios of 1:1, 1:2, and 2:1), nitric acid and hydrochloric acid. The study revealed that the adsorbed lead could be completely desorbed in the presence of mixed water/acetic acid solution with a volume ratio of 1:1. In this study, more than 98% of proposed lead could be desorbed and recovered by 1 mL of mixed water/acetic acid solution with a volume ratio of 1:1 in 25 min, when 0.45 mg Pb(II) (450 mL with a concentration of 1 mg/L) was already adsorbed on m-Fe₃O₄@ACCs. The reusability of the adsorbents in several successive separation processes was tested and the result showed that the m-Fe₃O₄@ACCs can be recycled and reused for seven times without significant reduction in its removal efficiency.

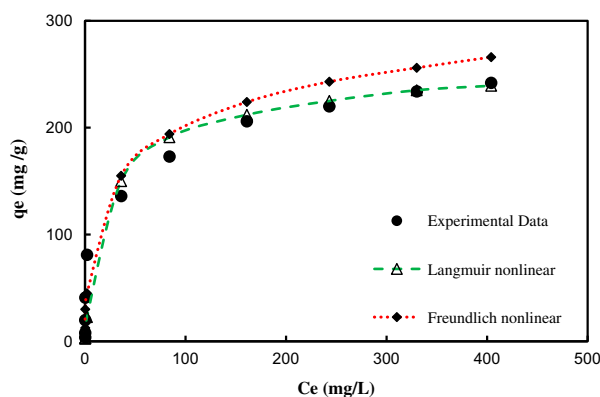


Fig. 9. Adsorption isotherms for Pb(II) on m-Fe₃O₄@ACCs at 298 K (nonlinear method).

Table 5

Langmuir and Freundlich constants for adsorption of Pb(II) onto m-Fe₃O₄@ACCs

Langmuir			Freundlich		
q_{max} (mg/g)	K_L (L/mg)	R^2	K_F (mg/g)	n	R^2
243.9	0.06	0.9939	26.45	2.49	0.713

Table 6

Comparison of adsorption capacity of various adsorbents for the removal of Pb(II)

Sorbent	q_m (mg/g)	Refs.
Magnetic Fe ₃ O ₄ -silica-xanthan gum composite	21.32	[8]
Amino-functionalized Fe ₃ O ₄ magnetic nano-particles	40.1	[6]
Kaolinite clay modified with 3-chloropropyltriethoxysilane	54.35	[63]
Combination of natural zeolite-kaolin bentonite	141	[58]
Magnetic hydrogels	126.4	[64]
Magnetic nanocomposite beads-chitosan	63.33	[65]
Algae	251	[66]
Peat	155	[66]
Iron oxide coated sewage sludge	42.4	[67]
Ethylenediamine modified attapulgite	100	[68]
Fe(III)-modified zeolite	133	[69]
Ethylenediamine functionalized SBA-15	360	[70]
Nano-scale zero valent iron	50.31	[71]
Combination of natural zeolite-kaolin-bentonite	140.9	[58]
Nanoparticles (NPs) suspensions of CeO ₂	189	[72]
Activated carbon	13.05	[73]
Zeolite tuff	34.48	[62]
m-Fe ₃ O ₄ @ACCs	243.9	This work

4. Conclusion

In this study, magnetic-activated carbon nanocomposite (m-Fe₃O₄@ACCs), as a novel magnetic nanocomposite was fabricated by using activated carbon and Fe₃O₄ nanoparticles which was characterized by TEM, VSM, and TGA analysis. The m-Fe₃O₄@ACCs nanocomposite was quite efficient as a magnetic nanocomposite for the fast removal of lead from aqueous solutions. Magnetic nanoparticles have potential application in the treatment of wastewater containing heavy metal such as lead. Low cost, short contact time, high adsorption capacity, stability, and reusability are advantages of m-Fe₃O₄@ACCs as adsorbent. The time required to achieve the adsorption equilibrium was 15 min. The adsorption of lead on the surface of m-Fe₃O₄@ACCs was concluded to be attributed to the electrostatic and hydrophobic interaction between cationic complexes (PAR-Pb²⁺ and Pb(NH₃)₄²⁺) and negative surface charge of adsorbent. The adsorption data followed the Langmuir isotherm equation and the maximum adsorption capacity on m-Fe₃O₄@ACCs was 243.9 mg/g. It also indicated that the adsorption was chemical adsorption process. Two adsorption kinetic models have been applied to fit the experimental data and pseudo-second-order was proved to be the best kinetic model.

In addition, 1 mL water/acetic acid solution with a volume ratio of 1:1 in 25 min was suitable for desorption lead ion and the reusability of m-Fe₃O₄@ACCs was for seven times. Importantly, more than 99% of Pb(II)

could be removed by m-Fe₃O₄@ACCs from industrial wastewater and tap water. Therefore, the magnetic activated carbon nanocomposite (m-Fe₃O₄@ACCs) could be regarded as a potential candidate for high efficient and renewable adsorbent for Pb(II) ions.

References

- [1] B. Yang, Q. Gong, L. Zhao, H. Sun, N. Ren, J. Qin, J. Xu, H. Yang, Preconcentration and determination of lead and cadmium in water samples with a MnO₂ coated carbon nanotubes by using ETAAS, *Desalination* 278 (2011) 65–69.
- [2] Z. Bahadır, V.N. Bulut, D. Ozdes, C. Duran, H. Bektas, M. Soylak, Separation and preconcentration of lead, chromium and copper by using with the combination coprecipitation-flame atomic absorption spectrometric determination, *J. Ind. Eng. Chem.* 20 (2014) 1030–1034.
- [3] M. Machida, T. Mochimaru, H. Tatsumoto, Lead(II) adsorption onto the graphene layer of carbonaceous materials in aqueous solution, *Carbon* 44 (2006) 2681–2688.
- [4] M. Soylak, E. Yilmaz, Ionic liquid dispersive liquid-liquid microextraction of lead as pyrrolidinedithiocarbamate chelate prior to its flame atomic absorption spectrometric determination, *Desalination* 275 (2011) 297–301.
- [5] M. Khajeh, Response surface modelling of lead preconcentration from food samples by miniaturised homogenous liquid-liquid solvent extraction: Box-Behnken design, *Food Chem.* 129 (2011) 1832–1838.
- [6] Y. Tan, M. Chen, Y. Hao, High efficient removal of Pb(II) by amino-functionalized Fe₃O₄ magnetic nanoparticles, *Chem. Eng. J.* 191 (2012) 104–111.

- [7] A. Abbas, A.M. Al-Amer, T. Laoui, M.J. Al-Marri, M.S. Nasser, M. Khraisheh, M.A. Atieh, Heavy metal removal from aqueous solution by advanced carbon nanotubes: Critical review of adsorption applications, *Sep. Purif. Technol.* 157 (2016) 141–161.
- [8] X. Peng, F. Xu, W. Zhang, J. Wang, C. Zeng, M. Niu, E. Chmielewska, Magnetic Fe₃O₄@silica-xanthan gum composites for aqueous removal and recovery of Pb²⁺, *Colloids Surf., A* 443 (2014) 27–36.
- [9] S. Ogawa, M. Katoh, T. Sato, Contribution of hydroxypatite and ferrihydrite in combined applications for the removal of lead and antimony from aqueous solutions, *Water, Air, Soil Pollut.* 225 (2014) 1–12.
- [10] L. Argüello, A.R. Hernandez-Martínez, A. Rodríguez, G.A. Molina, R. Esparza, M. Estevez, Novel chitosan/polyurethane/anatase titania porous hybrid composite for removal of metal ions waste, *J. Chem. Technol. Biotechnol.* (2016), doi: 10.1002/jctb.4945.
- [11] N. Wang, X. Xu, H. Li, J. Zhai, L. Yuan, K. Zhang, H. Yu, Preparation and application of a xanthate-modified thiourea chitosan sponge for the removal of Pb(II) from aqueous solutions, *Ind. Eng. Chem. Res.* 55(17) (2016) 4960–4968.
- [12] D. Jia, C. Li, Adsorption of Pb(II) from aqueous solutions using corn straw, *Desalin. Water Treat.* 56(1) (2015) 223–231.
- [13] P. Geetha, M. Latha, S.S. Pillai, M. Koshy, Nanoalginate based biosorbent for the removal of lead ions from aqueous solutions: Equilibrium and kinetic studies, *Ecotoxicol. Environ. Saf.* 122 (2015) 17–23.
- [14] C.-S. Zhu, X. Dong, L.-P. Wang, Removal of Pb(II), Cu(II), and Zn(II) from aqueous solutions by amorphous Tin(IV) hydrogen phosphate immobilized on silica, *Water, Air, Soil Pollut.* 225 (2014) 1–10.
- [15] I. Zawierucha, C. Kozłowski, G. Malina, Immobilized materials for removal of toxic metal ions from surface/groundwaters and aqueous waste streams, *Environ. Sci.: Process. Impacts* 18 (2016) 429–444.
- [16] M. Liu, Y. Sun, S. Na, F. Yan, Selective adsorption of lead(II) from aqueous solution by ion-imprinted PEI-functionalized silica sorbent: Studies on equilibrium isotherm, kinetics, and thermodynamics, *Desalin. Water Treat.* 57(7) (2016) 3270–3282.
- [17] J. Wang, X. Li, Ion-imprinted poly(2-acrylamido-2-methyl-1-propanesulfonic acid)/modified silica composite hydrogel for selective and enhanced adsorption of Pb(II) ions, *Desalin. Water Treat.* 52 (2014) 274–282.
- [18] I.E.M. Carpio, J.D. Mangadlao, H.N. Nguyen, R.C. Advincula, D.F. Rodrigues, Graphene oxide functionalized with ethylenediamine triacetic acid for heavy metal adsorption and anti-microbial applications, *Carbon* 77 (2014) 289–301.
- [19] M. Yari, M. Norouzi, A.H. Mahvi, M. Rajabi, A. Yari, O. Moradi, I. Tyagi, V.K. Gupta, Removal of Pb(II) ion from aqueous solution by graphene oxide and functionalized graphene oxide-thiol: Effect of cysteamine concentration on the bonding constant, *Desalin. Water Treat.* 57(24) (2015) 11195–11210.
- [20] J.-G. Yu, L.-Y. Yu, H. Yang, Q. Liu, X.-H. Chen, X.-Y. Jiang, X.-Q. Chen, F.-P. Jiao, Graphene nanosheets as novel adsorbents in adsorption, preconcentration and removal of gases, organic compounds and metal ions, *Sci. Total Environ.* 502 (2015) 70–79.
- [21] İ. Duru, D. Ege, A.R. Kamali, Graphene oxides for removal of heavy and precious metals from wastewater, *J. Mater. Sci.* 51 (2016) 6097–6116.
- [22] M.J. Amiri, J. Abedi-Koupai, S.S. Eslamian, M. Arshadi, Adsorption of Pb(II) and Hg(II) ions from aqueous single metal solutions by using surfactant-modified ostrich bone waste, *Desalin. Water Treat.* 57 (35) (2015) 16522–16539.
- [23] H. Lu, X. Qiao, W. Wang, F. Tan, Z. Xiao, J. Chen, Facile preparation of mesoporous silica/nano zero-valent iron composite for Pb(II) removal from aqueous solution, *Desalin. Water Treat.* 57(23) (2015) 10745–10756.
- [24] Y. Cheng, C. Jiao, W. Fan, Synthesis and characterization of coated zero-valent iron nanoparticles and their application for the removal of aqueous Pb²⁺ ions, *Desalin. Water Treat.* 54 (2015) 502–510.
- [25] J. Haiyan, Z. Qiuxiang, Z. Ying, Removal of Cd(II) and Pb(II) from aqueous solutions by modified polyvinyl alcohol, *Desalin. Water Treat.* 57(14) (2016) 6452–6462.
- [26] D.d.Q. Melo, C.B. Vidal, T.C. Medeiros, G.S.C. Raulino, A. Dervanoski, M.d.C. Pinheiro, R.F.d. Nascimento, Biosorption of metal ions using a low cost modified adsorbent (*Mauritia flexuosa*): Experimental design and mathematical modeling, *Environ. Technol.* (2016) 1–15, doi: 10.1080/09593330.2016.1144796.
- [27] B.O. Jones, O.O. John, C. Luke, A. Ochieng, B.J. Basse, Application of mucilage from *Dicerocaryum eriocarpum* plant as biosorption medium in the removal of selected heavy metal ions, *J. Environ. Manage.* 177 (2016) 365–372.
- [28] S. Mallakpour, M. Madani, Functionalized-MnO₂/chitosan nanocomposites: A promising adsorbent for the removal of lead ions, *Carbohydr. Polym.* 147 (2016) 53–59.
- [29] F. Wang, X. Lu, X.-Y. Li, Selective removals of heavy metals (Pb²⁺, Cu²⁺, and Cd²⁺) from wastewater by gelation with alginate for effective metal recovery, *J. Hazard. Mater.* 308 (2016) 75–83.
- [30] R. Li, M. Zhang, Y. Yang, Z. Zhang, R. Qin, L. Wang, J. Zheng, X. Sun, Adsorption of Pb(II) ions in aqueous solutions by common reed ash-derived SBA-15 modified by amino-silanes, *Desalin. Water Treat.* 55(6) (2015) 1554–1566.
- [31] S. Hokkanen, A. Bhatnagar, M. Sillanpää, A review on modification methods to cellulose-based adsorbents to improve adsorption capacity, *Water Res.* 91 (2016) 156–173.
- [32] G. Zhou, J. Luo, C. Liu, L. Chu, J. Ma, Y. Tang, Z. Zeng, S. Luo, A highly efficient polyampholyte hydrogel sorbent based fixed-bed process for heavy metal removal in actual industrial effluent, *Water Res.* 89 (2016) 151–160.
- [33] H. Alijani, M.H. Beyki, Z. Shariatnia, M. Bayat, F. Shemirani, A new approach for one step synthesis of magnetic carbon nanotubes/diatomite earth composite by chemical vapor deposition method: Application for removal of lead ions, *Chem. Eng. J.* 253 (2014) 456–463.
- [34] M.A. Salam, R.M. El-Shishtawy, A.Y. Obaid, Synthesis of magnetic multi-walled carbon nanotubes/magnetite/chitin magnetic nanocomposite for the removal of Rose Bengal from real and model solution, *J. Ind. Eng. Chem.* 20 (2014) 3559–3567.

- [35] V. Gupta, O. Moradi, I. Tyagi, S. Agarwal, H. Sadegh, R. Shahryari-Ghoshekandi, A. Makhlof, M. Goodarzi, A. Garshasbi, Study on the removal of heavy metal ions from industry waste by carbon nanotubes: Effect of the surface modification: A review, *Crit. Rev. Environ. Sci. Technol.* 46 (2016) 93–118.
- [36] N.M. Mubarak, M. Thobashinni, E.C. Abdullah, J.N. Sahu, Comparative kinetic study of removal of Pb^{2+} ions and Cr^{3+} ions from waste water using carbon nanotubes produced using microwave heating, *Carbon* 7 (2016) 2–16.
- [37] N.M.M. Fourier, J.N. Sahu, E.C. Abdullah, N.S. Jayakumar, Rapid adsorption of toxic Pb(II) ions from aqueous solution using multiwall carbon nanotubes synthesized by microwave chemical vapor deposition technique, *J. Environ. Sci.* (2016), doi: [10.1016/j.jes.2015.12.025](https://doi.org/10.1016/j.jes.2015.12.025).
- [38] Z.-j. Yi, J. Yao, H.-l. Chen, F. Wang, X. Liu, J.-s. Xu, Equilibrium and kinetic studies on adsorption of Pb(II) by activated palm kernel husk carbon, *Desalin. Water Treat.* 57(16) (2015) 7245–7253.
- [39] M. Imamoglu, H. Şahin, Ş. Aydın, F. Tosunoğlu, H. Yılmaz, S.Z. Yıldız, Investigation of Pb(II) adsorption on a novel activated carbon prepared from hazelnut husk by K_2CO_3 activation, *Desalin. Water Treat.* 57(10) (2016) 4587–4596.
- [40] S. Salehin, A.S. Aburizaiza, M. Barakat, Activated carbon from residual oil fly ash for heavy metals removal from aqueous solution, *Desalin. Water Treat.* 57 (2016) 278–287.
- [41] H.-Y. Zhu, Y.-Q. Fu, R. Jiang, J.-H. Jiang, L. Xiao, G.-M. Zeng, S.-L. Zhao, Y. Wang, Adsorption removal of congo red onto magnetic cellulose/ Fe_3O_4 /activated carbon composite: Equilibrium, kinetic and thermodynamic studies, *Chem. Eng. J.* 173 (2011) 494–502.
- [42] X. Luo, L. Zhang, High effective adsorption of organic dyes on magnetic cellulose beads entrapping activated carbon, *J. Hazard. Mater.* 171 (2009) 340–347.
- [43] H. Zhu, R. Jiang, L. Xiao, G. Zeng, Preparation, characterization, adsorption kinetics and thermodynamics of novel magnetic chitosan enwrapping nano-sized $\gamma-Fe_2O_3$ and multi-walled carbon nanotubes with enhanced adsorption properties for methyl orange, *Bioresour. Technol.* 101 (2010) 5063–5069.
- [44] J. Zhang, J.-L. Gong, G.-M. Zeng, X.-M. Ou, Y. Jiang, Y.-N. Chang, M. Guo, C. Zhang, H.-Y. Liu, Simultaneous removal of humic acid/fulvic acid and lead from landfill leachate using magnetic graphene oxide, *Appl. Surf. Sci.* 370 (2016) 335–350.
- [45] X. Bao, Z. Qiang, J.-H. Chang, W. Ben, J. Qu, Synthesis of carbon-coated magnetic nanocomposite ($Fe_3O_4@C$) and its application for sulfonamide antibiotics removal from water, *J. Environ. Sci.* 26 (2014) 962–969.
- [46] M. Tahergorabi, A. Esrafil, M. Kermani, M. Shirzad-Siboni, Application of thiol-functionalized mesoporous silica-coated magnetite nanoparticles for the adsorption of heavy metals, *Desalin. Water Treat.* (2015) 1–12, doi: [10.1080/19443994.2015.1106351](https://doi.org/10.1080/19443994.2015.1106351).
- [47] N. Erathodiyil, J.Y. Ying, Functionalization of inorganic nanoparticles for bioimaging applications, *Acc. Chem. Res.* 44 (2011) 925–935.
- [48] J. Ghasemi, H. Peyman, M. Meloun, Study of complex formation between 4-(2-Pyridylazo) Resorcinol and Al^{3+} , Fe^{3+} , Zn^{2+} , and Cd^{2+} ions in an aqueous solution at 0.1 M ionic strength, *J. Chem. Eng. Data* 52 (2007) 1171–1178.
- [49] F. Tajabadi, Y. Yamini, M.R. Sovizi, Carbon-based magnetic nanocomposites in solid phase dispersion for the preconcentration some of lanthanides, followed by their quantitation via ICP-OES, *Microchim. Acta* 180 (2013) 65–73.
- [50] J. Toniolo, A.S. Takimi, M.J. Andrade, R. Bonadiman, C.P. Bergmann, Synthesis by the solution combustion process and magnetic properties of iron oxide (Fe_3O_4 and $\alpha-Fe_2O_3$) particles, *J. Mater. Sci.* 42 (2007) 4785–4791.
- [51] S. Chatterjee, S.H. Woo, The removal of nitrate from aqueous solutions by chitosan hydrogel beads, *J. Hazard. Mater.* 164 (2009) 1012–1018.
- [52] S. Yadav, V. Srivastava, S. Banerjee, C.-H. Weng, Y.C. Sharma, Adsorption characteristics of modified sand for the removal of hexavalent chromium ions from aqueous solutions: Kinetic, thermodynamic and equilibrium studies, *Catena* 100 (2013) 120–127.
- [53] J. Zhang, Preparation, characterization and application of thiosemicarbazide grafted multiwalled carbon nanotubes for solid-phase extraction of Cd(II), Cu(II) and Pb(II) in environmental samples, *J. Environ. Sci.* 25 (2013) 2331–2337.
- [54] Y. Cengeloglu, A. Tor, M. Ersoz, G. Arslan, Removal of nitrate from aqueous solution by using red mud, *Sep. Purif. Technol.* 51 (2006) 374–378.
- [55] H. Elliott, C. Huang, The effect of complex formation on the adsorption characteristics of heavy metals, *Environ. Int.* 2 (1979) 145–155.
- [56] G. Absalan, M. Asadi, S. Kamran, L. Sheikhan, D.M. Goltz, Removal of reactive red-120 and 4-(2-pyridylazo) resorcinol from aqueous samples by Fe_3O_4 magnetic nanoparticles using ionic liquid as modifier, *J. Hazard. Mater.* 192 (2011) 476–484.
- [57] S. Baytak, A.R. Turker, Determination of lead and nickel in environmental samples by flame atomic absorption spectrometry after column solid-phase extraction on Ambersorb-572 with EDTA, *J. Hazard. Mater.* 129 (2006) 130–136.
- [58] A. Salem, R.A. Sene, Removal of lead from solution by combination of natural zeolite-kaolin-bentonite as a new low-cost adsorbent, *Chem. Eng. J.* 174 (2011) 619–628.
- [59] A. Çelekli, H. Bozkurt, Bio-sorption of cadmium and nickel ions using *Spirulina platensis*: Kinetic and equilibrium studies, *Desalination* 275 (2011) 141–147.
- [60] M.A. Tofighy, T. Mohammadi, Adsorption of divalent heavy metal ions from water using carbon nanotube sheets, *J. Hazard. Mater.* 185 (2011) 140–147.
- [61] A. Shamsizadeh, M. Ghaedi, A. Ansari, S. Azizian, M. Purkait, Tin oxide nanoparticle loaded on activated carbon as new adsorbent for efficient removal of malachite green-oxalate: Non-linear kinetics and isotherm study, *J. Mol. Liq.* 195 (2014) 212–218.
- [62] S.K.R. Yadanaparthi, D. Graybill, R. von Wandruszka, Adsorbents for the removal of arsenic, cadmium, and lead from contaminated waters, *J. Hazard. Mater.* 171 (2009) 1–15.
- [63] M. Al-Harabsheh, R. Shawabkeh, A. Al-Harabsheh, K. Tarawneh, M.M. Batiha, Surface modification and characterization of Jordanian kaolinite: Application for lead removal from aqueous solutions, *Appl. Surf. Sci.* 255 (2009) 8098–8103.

- [64] O. Ozay, S. Ekici, Y. Baran, N. Aktas, N. Sahiner, Removal of toxic metal ions with magnetic hydrogels, *Water Res.* 43 (2009) 4403–4411.
- [65] H.V. Tran, L. Dai Tran, T.N. Nguyen, Preparation of chitosan/magnetite composite beads and their application for removal of Pb(II) and Ni(II) from aqueous solution, *Mater. Sci. Eng.: C* 30 (2010) 304–310.
- [66] Y. Ho, G. McKay, Batch lead(II) removal from aqueous solution by peat, *Process Saf. Environ. Prot.* 77 (1999) 165–173.
- [67] T. Phuengprasop, J. Sittiwong, F. Unob, Removal of heavy metal ions by iron oxide coated sewage sludge, *J. Hazard. Mater.* 186 (2011) 502–507.
- [68] Y. Deng, Z. Gao, B. Liu, X. Hu, Z. Wei, C. Sun, Selective removal of lead from aqueous solutions by ethylenediamine-modified attapulgite, *Chem. Eng. J.* 223 (2013) 91–98.
- [69] M. Kragović, A. Daković, Ž. Sekulić, M. Trgo, M. Ugrina, J. Perić, G.D. Gatta, Removal of lead from aqueous solutions by using the natural and Fe(III)-modified zeolite, *Appl. Surf. Sci.* 258 (2012) 3667–3673.
- [70] L. Hajiaghababaei, A. Badii, M.R. Ganjali, S. Heydari, Y. Khaniani, G.M. Ziarani, Highly efficient removal and preconcentration of lead and cadmium cations from water and wastewater samples using ethylenediamine functionalized SBA-15, *Desalination* 266 (2011) 182–187.
- [71] N. Arancibia-Miranda, S.E. Baltazar, A. García, A.H. Romero, M.A. Rubio, D. Altbir, Lead removal by nano-scale zero valent iron: Surface analysis and pH effect, *Mater. Res. Bull.* 59 (2014) 341–348.
- [72] S. Recillas, A. García, E. González, E. Casals, V. Puentes, A. Sánchez, X. Font, Use of CeO₂, TiO₂ and Fe₃O₄ nanoparticles for the removal of lead from water, *Desalination* 277 (2011) 213–220.
- [73] M. Imamoglu, O. Tekir, Removal of copper(II) and lead(II) ions from aqueous solutions by adsorption on activated carbon from a new precursor hazelnut husks, *Desalination* 228 (2008) 108–113.